JOURNAL OF AGRICULTURAL AND FOOD CHEMISTRY
ARTICLE

J. Agric. Food Chem. 2010, 58, 6131–6140 6131
DOI:10.1021/jf903598w

Glucose Reversion Reaction Kinetics

Heidi M. Pilath,*,† Mark R. Nimlos,† Ashutosh Mittal,§ Michael E. Himmel,§ and David K. Johnson§

†National Bioenergy Center, and §Biosciences Center, National Renewable Energy Laboratory, Golden, Colorado 80401

The reversion reactions of glucose in mildly acidic aqueous solutions have been studied, and the kinetics of conversion to disaccharides has been modeled. The experiments demonstrate that, at high sugar loadings, up to 12 wt % of the glucose can be converted into reversion products. The reversion products observed are primarily disaccharides; no larger oligosaccharides were observed. Only disaccharides linked to the C1 carbon of one of the glucose residues were observed. The formation of 1,6-linked disaccharides was favored, and α-linked disaccharides were formed at higher concentrations than β-linked disaccharides. This observation can be rationalized on the basis of steric effects. At temperatures >140 °C, the disaccharides reach equilibrium with glucose and the reversion reaction competes with dehydration reactions to form 5-hydroxymethylfurfural. As a result, disaccharide formation reaches a maximum at reaction times <10 min and decreases with time. At temperatures <130 °C, disaccharide formation reaches a maximum at reaction times >30 min. As expected, disaccharide formation exhibits a second-order dependence upon glucose concentration. Levoglucosan formation is also observed; because it shows a first-order dependence upon glucose concentration, its formation is more significant at low concentrations (10 mg mL^{-1}), whereas disaccharide formation dominates at high concentrations (200 mg mL^{-1}). Experiments conducted using glucose and its disaccharides were calibrated with readily available standards. The kinetic parameters for hydrolysis of some glucodisaccharides could be compared to published literature values. From these experiments, the kinetics and activation energies for the reversion reactions have been calculated. The rate parameters can be used to model the formation of the disaccharides as a function of reaction time and temperature. A new and detailed picture of the molecular mechanism of these industrially important reversion reactions has been developed.

KEYWORDS: Glucose; cellobiose; glucodisaccharides; glucooligomers; sugar loss; reversion reactions; anhydroglucose; levoglucosan

INTRODUCTION

Reversion reactions (*1*−*12*) of glucose, **1**, result in the formation of oligosaccharides or anhydrosugars from the acid-catalyzed reactions of the monomer. These reactions are important in food processing (*13*) and in the conversion of biomass to fuels and chemicals (*2*, *8*). Such reactions result in a loss of monosaccharide (glucose), which is the desired product from these processes. Most previous work concerning the formation of reversion products was performed and reported prior to 1965 and involved the reactions of glucose from starch during the production of corn syrups. More recently, reversion reactions have been of interest in the production of renewable transportation fuels from biomass (*10*−*12*). Acid-catalyzed hydrolysis of hemicellulose and cellulose can be used to prepare monosaccharides, which can be used as feedstocks for fermentation or as starting materials for additional processing. In these processes, it is often advantageous to use high biomass loadings so that high-concentration sugar solutions (i.e., > 200 mg mL^{-1}) result. Unfortunately, under these conditions, catalyzed self-reactions of the monomers, that is, reversion reactions, are possible. The oligosaccharides resulting from reversion reactions are often difficult to further process (ferment), and as a result, it is of interest to understand the kinetics of these reactions so that hydrolysis can be optimized for monosaccharide production.

The reaction mechanisms for reversion reactions involve the formation of an intermediate carbocation at the C1 carbon atom of glucose. Reaction 1 shows the formation of the carbocation from proton addition to the C1 hydroxyl group and subsequent loss of a water molecule. This hydroxyl group has the largest affinity for protons, and the resulting carbocation is stabilized by the oxonium ion resonance structure. The hydroxyl group of another sugar molecule can then add to the carbocation to form a disaccharide. Because the carbocation is essentially flat, the hydroxyl group can add to either side and the stereochemistry of the anomeric C1 is scrambled. For example, reactions 2 and 3 show the addition of the C1 atom on a β-glucose molecule to the carbocation, forming the disaccharide neotrehalose (α addition) or isotrehalose (β addition), respectively. Addition of α-glucose, which is in equilibrium with β-glucose, to the carbocation results in the formation of both neotrehalose and trehalose. Likewise, addition of the other hydroxyl groups to the carbocation can form α and β isomers of 1,6-, 1,4-, 1,3- and 1,2-linked disaccharides for a total of 11 different disaccharides resulting from 2 glucopyranose units. Table S1 in the Supporting Information shows the possible disaccharide products from

*Corresponding author: Email address: heidi.pilath@nrel.gov.

Published on Web 04/29/2010

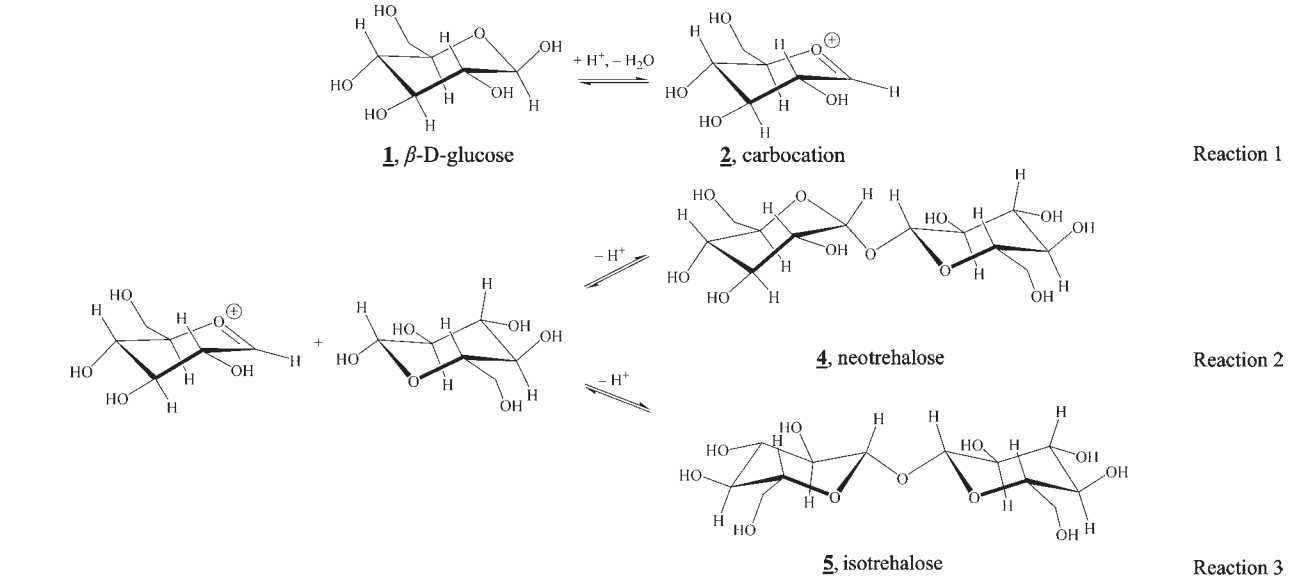

the reversion reaction of glucose. Because this reversion reaction is bimolecular, one could expect a second-order reaction in terms of glucose concentration. Thus, this reaction becomes more important as the process is conducted at higher substrate loadings.

The yield of reversion products is a function of the reactivity of an individual hydroxyl group toward the carbocation as well as the stability of the glycosidic bond that is formed (*7*). The C6 hydroxyl group is the most reactive in the glucose molecule and forms the most stable glycosidic bond. It has been experimentally shown that the two most prominent products are the 1,6-linked disaccharides (*1*, *3*, *5*). This is likely due to reduced steric hindrance between the bulky sugar rings when there is an additional methylene group in the linkage (*5*).

In addition to the bimolecular reversion reactions, the carbocations formed in reaction 1 can also undergo an internal ring closure to form anhydrosugars, which can constitute a significant fraction of the reversion products formed. This is shown in reaction 4 for the glucose cation resulting in the formation of a pyranosyl anhydrosugar, 1,6-anhydro-β-D-glucopyranose (**14**, levoglucosan). In addition to levoglucosan (*3*, *5*), the formation of 1,6-anhydro-β-D-glucofuranose, **17**, from glucose has been reported in the literature (*14*, *15*). This product can be formed by an analogous mechanism involving the glucofuranose, **15**, and the furanyl carbocation, **16**, as shown in reactions 5 and 6.

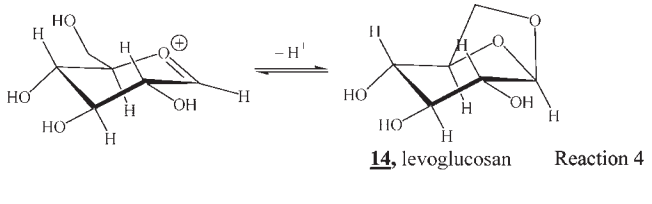

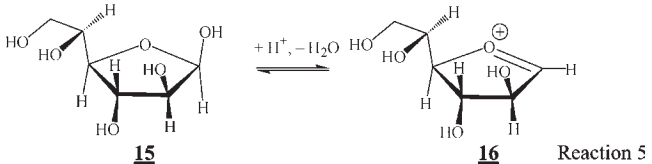

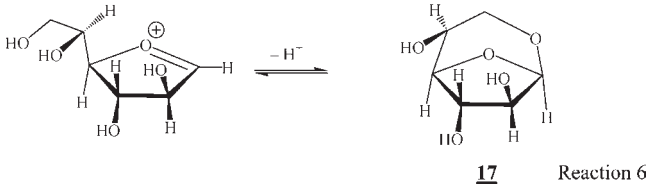

Knowledge of the rates of these reversion reactions will be important for optimizing starch and cellulosic conversion processes. To predict the formation of these unwanted byproducts, the kinetics and energetics of these reactions are needed, yet there is a limited amount of these data in the literature. There have been experimental measurements on the enthalpy, free energy, and activation energy for the reverse of these reactions, that is, hydrolysis of some of the disaccharides. Goldberg and co-workers measured the equilibrium concentrations of 1,6-linked disaccharides and glucose by enzymatically treating the disaccharides with hydrolase enzymes (*16*−*18*). From these measurements, they derived equilibrium constants as a function of temperature and free energies and enthalpies of hydrolysis. Kinetic studies of the hydrolysis of many of the disaccharides in 0.01 M hydrochloric acid were used to derive activation energies for these reactions. These results are presented in **Table 1**. However, this collection of data is insufficient to develop kinetic models for all of the reversion reactions that are possible during the hydrolysis of cellulose or starch.

In this paper, the formation of reversion reaction products in mildly acidic solutions of glucose has been studied, and kinetic models to describe the formation of nearly all of the important reversion products have been developed. Experiments were conducted in a robotic microwave-heated reactor system, and the products were measured using high-performance liquid chromatography (HPLC) as well as anion exchange chromatography. In addition to direct measurements of reversion reactions starting with glucose, the hydrolysis of several glucodisaccharides and the formation and hydrolysis of levoglucosan were independently measured. An Arrhenius rate formulation was used to fit kinetic models to experimental measurements obtained at different temperatures.

MATERIALS AND METHODS

Batch reaction experiments with glucose, glucodisaccharide, and levoglucosan solutions were performed using a microwave reactor (Explorer, CEM Corp., Matthews, NC) outfitted with a 48-position autosampler. Microwave frequency radiation of 230 MHz with a maximum pulsed radiation power of 200 W was used to heat the samples. Reactions were carried out in sealed 10 mL reactor tubes containing 2 mL of the carbohydrate in an aqueous solution of sulfuric acid (1.2 wt % H_2SO_4). Solutions were continuously stirred during the experiments so as to ensure uniform heating. The temperature inside the reactor was monitored by measuring the infrared emission from the bottom of the tube, and pressure was measured with a transducer at the top of the reactor.

Table 1. Literature Values for Hydrolysis of Glucose Disaccharides[a]

common name	IUPAC name	$\Delta_r G°$ (kJ mol^{-1})	$\Delta_r H°$ (kJ mol^{-1})	E_a (kJ mol^{-1})
3, trehalose	1,1-α-D-glucopyranosyl-α-D-glucopyranoside	−11.9[b]	−4.73[b]	168.1[c]
4, neotrehalose	1,1-α-D-glucopyranosyl-β-D-glucopyranoside			
5, isotrehalose	1,1-β-D-glucopyranosyl-β-D-glucopyranoside			
6, kojibiose	1,2-*O*-α-D-glucopyranosyl-D-glucose			138.9[d]
7, sophorose	1,2-*O*-β-D-glucopyranosyl-D-glucose			120.9[d]
8, nigerose	1,3-*O*-α-D-glucopyranosyl-D-glucose			113.8[d]
9, laminaribiose	1,3-*O*-β-D-glucopyranosyl-D-glucose			125.6[d]
10, maltose	1,4-*O*-α-D-glucopyranosyl-D-glucose	−15.65[e]	−4.02[e]	132.0[d]
				129.6[f]
11, cellobiose	1,4-*O*-β-D-glucopyranosyl-D-glucose	≤−12.5[g]	−2.43[g]	129.0[d]
				128.4[f]
				130.0[h]
12, isomaltose	1,6-*O*-α-D-glucopyranosyl-D-glucose	−7.1[i]	5.86[i]	141.0[d]
13, gentiobiose	1,6-*O*-β-D-glucopyranosyl-D-glucose	−7.1[i]	2.58[i]	141.2[d]
				139.7[e]

[a] The thermodynamic values are for the hydrolysis of the disaccharide (i.e., disaccharide + water molecule → 2 glucose molecules). [b] Reference *18*. [c] Reference *20*. [d] Reference *13*. [e] References *16*, *17*, and *19*. [f] Reference *21*. [g] References *17* and *19*. [h] Reference *22*. [i] Reference *17*.

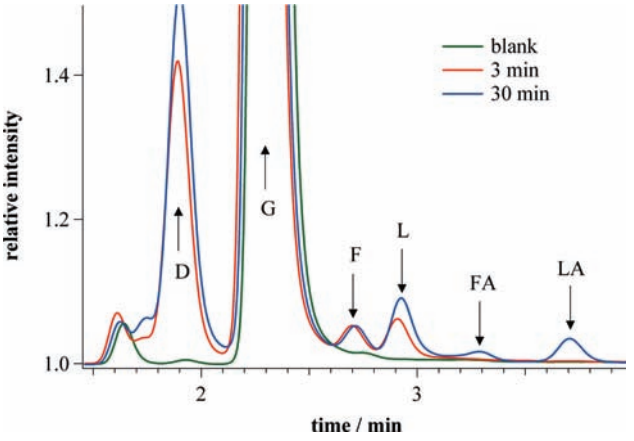

Figure 1. Typical HPLC chromatogram of products from the reaction of glucose (200 mg mL^{-1}) in 1.2 wt % H_2SO_4. The calibrated peak for levoglucosan (L) is shown, as is a tentative assignment of 1,6-anhydro-β-D-glucofuranose (F) at 120 °C. The peaks for glucose (G), glucodisaccharides (D), formic acid (FA), and levulinic acid (LA) are also shown.

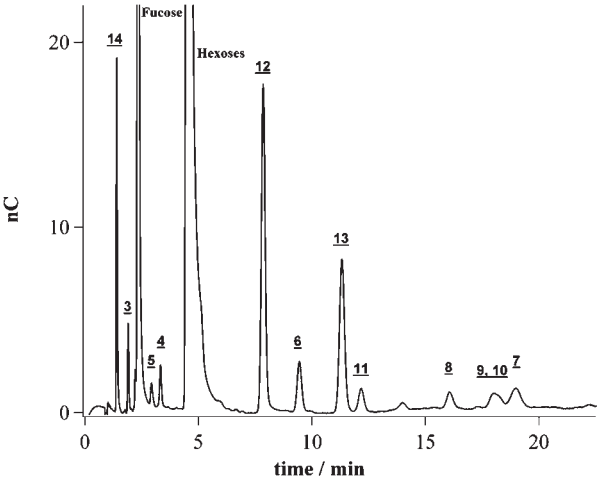

Figure 2. Typical anion chromatogram of the products from the reaction of glucose (200 mg mL^{-1}) in 1.2 wt % H_2SO_4 at 120 °C. Fucose was the internal standard. Refer to **Table 1** for the identities of the numbered peaks, except for peak 14 which is levoglucosan.

A computer-controlled temperature and pressure feedback system was used to regulate the microwave power for rapid heating and constant temperature. For pressure feedback, values were read into the software that then applied an algorithm to control pressure. Steam table pressures were used to validate target temperatures. Samples were cooled via a stream of compressed air that was blown on the reactor tubes at the end of each run. For each temperature studied, control methods for the microwave reactor were developed to minimize heat-up time, reduce overshoot, and provide a steady target temperature. Temperature, pressure, and microwave power profiles were acquired and stored for each experiment using reactor control software (Synergy, CEM Corp.). A typical CEM temperature/pressure plot can be found in the Supporting Information. The reactor was rapidly heated (within 2 min) to the target temperature, and the temperature was maintained to within 1 °C throughout the experiment.

The solutions were analyzed using an HPLC with refractive index and photodiode array detectors (Agilent 1100, Agilent Technologies, Palo Alto, CA). A Rezex RFQ Fast Acids column (100 × 7.8 mm, 8 μm particle size, Phenomenex, Torrance, CA) and Cation H+ guard column (Bio-Rad Laboratories, Hercules, CA) operated at 85 °C were used to separate sugar monomers, total oligomers, and degradation products present in the reaction solutions. The eluent was 0.02 M H_2SO_4 with a flow rate of 1.0 mL min^{-1}. Samples and standards were filtered through a 0.45 μm nylon membrane syringe filter (Pall Corp., East Hills, NY) prior to injection (2.5 μL) onto the column. Calibration standards (Absolute Standards, Inc., New Haven, CT), consisting of a suite of 11 sugar monomers, cellobiose, and the degradation products 5-hydroxymethylfurfural (5-HMF) and furfural, were used in addition to levoglucosan, which was synthesized in-house. No commercial standard currently exists for 1,6-anhydro-β-D-glucofuranose. A concentration verification standard (CVS), also prepared by Absolute Standards, was used to periodically check detector response. Triplicates were run at various reaction times within each experiment and the standard deviations are indicated by the error bars. The HPLC was controlled and data were analyzed using Agilent Chemstation software (Rev. A.09.03). **Figure 1** shows a typical plot of a portion of a chromatogram obtained from the reaction of a 200 mg mL^{-1} glucose solution at 120 °C. As can be seen, the peak for glucose (retention time, RT = 2.33 min) was resolved from that for levoglucosan (RT = 2.9 min) and a peak tentatively identified as 1,6-anhydro-β-D-glucofuranose, **17** (RT = 2.7 min). The peak at a retention time of 1.9 min contained all of the oligosaccharides. 5-HMF was also measured with this apparatus, and this species eluted much later, at approximately 9.5 min. The eluent peak had a retention time of 1.62 min. At reaction times of 30 min or greater 2 additional peaks were observed

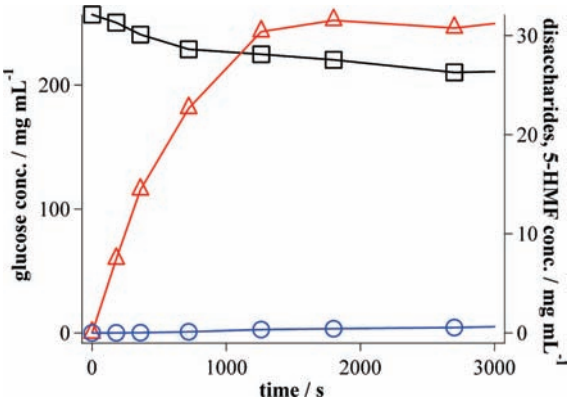

Figure 3. Typical results for the reaction of glucose (black squares) to give total disaccharides (red triangles) and 5-HMF (blue circles) as measured by HPLC. Batch experiments were conducted at 140 °C with 300 mg mL^{-1} glucose in 1.2 wt % H_2SO_4.

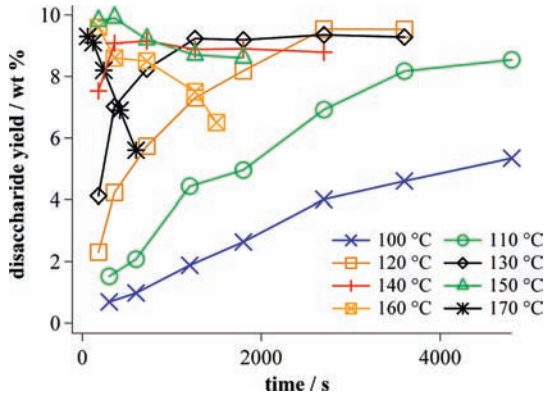

Figure 4. Formation of total disaccharides as a function of reaction time for different reactor temperatures. The starting concentration of glucose was 200 mg mL^{-1} in 1.2 wt % H_2SO_4.

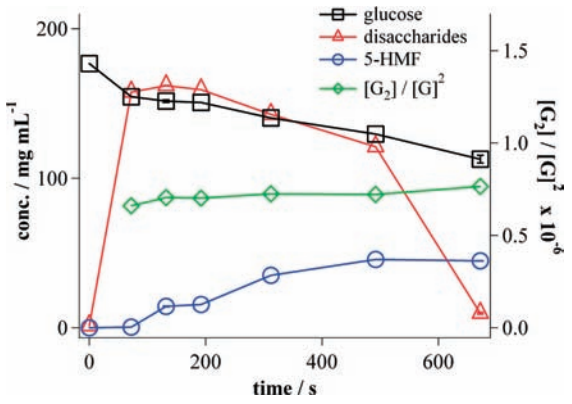

Figure 5. Concentrations of glucose (black squares), disaccharides (multiplied by 10, red triangles), 5-HMF (multiplied by 10, blue circles), and equilibrium ratio of disaccharides/$(glucose)^2$ (green diamonds), as a function of reaction time at 170 °C. The starting glucose concentration was 200 mg mL^{-1}, and the concentration of H_2SO_4 was 1.2 wt %.

due to the 5-HMF degradation products, formic acid (RT = 3.3 min) and levulinic acid (RT = 3.7 min).

To resolve the oligosaccharide products, solutions were analyzed by anion chromatography (Dionex DX-600, Dionex Corp., Sunnyvale, CA) on a CarboPac PA-20 column (3 × 150 mm, Dionex Corp.) operated at 35 °C. Optimal separation was achieved by gradient elution with the eluent increasing from 25 mM potassium hydroxide (KOH) to 100 mM KOH linearly over 20 min. It was held for an additional 5 min to regenerate the column and then re-equilibrated at the starting eluent composition for 5 min at the end of each run. Solute concentrations were measured with an ED50 electrochemical detector operated with waveform A. The chromatograph was controlled and the data were analyzed using Dionex Chromeleon software (V 6.8). Pure standards were available for all of the glucose-derived reversion products, with the exception of 1,6-anhydro-β-D-glucofuranose. Samples and standards were diluted to a maximum concentration of approximately 4 mg L^{-1} with a diluent that included fucose (6 mg L^{-1}) as an internal standard and sodium azide (0.04 wt %) as a preservative. **Figure 2** shows a typical chromatogram measured from a reaction with glucose. This chromatogram shows that all of the possible disaccharides (refer to Table S1 in the Supporting Information) were resolved, with the exception of laminaribiose, **9**, and maltose, **10**. Laminaribiose appears as a shoulder on the maltose peak and has not been quantified in this study. As will be discussed later, the peaks for the 1,6-linked disaccharides (isomaltose, **12**, and gentiobiose, **13**) are significantly larger than for the other disaccharides. In size exclusion experiments conducted by Minor (*2*), evidence for trisaccharide formation came by way of a shoulder on a disaccharide peak. In our experiments, trisaccharide formation was significantly lower than that of any disaccharide, and their contribution to overall oligomers was neglected.

RESULTS AND DISCUSSION

Temperature Dependence. Initial reactants formed from the reversion reactions of glucose were analyzed using the Agilent HPLC described above, which allowed measurement of the total amount of oligomers formed. As was demonstrated later with anion exchange chromatography (**Figure 2**), disaccharides were predominantly detected during these experiments, and so we treated the total oligomer peak measured with the Agilent HPLC as disaccharides. A cellobiose standard was then used to calibrate the peak to estimate the total yield of disaccharide products. This approximation was justified due to the similar response factors for all of the disaccharides on the refractive index detector, and as shown in **Figure 2**, larger oligosaccharides were not detected. The value obtained for total disaccharides concentration from this calibration was similar to the sum of the individual disaccharide concentrations obtained from the anion exchange instrument. **Figure 3** shows typical data for the reaction of glucose to produce disaccharides at 140 °C starting with 300 mg mL^{-1} glucose. The plot shows that while the glucose concentration decreased, the disaccharide concentration increased until a reaction time of about 2000 s. At this point the disaccharide and glucose concentrations became constant, suggesting that the reversion reactions had reached equilibrium.

The concentration of 5-HMF, **18**, is also plotted as a function of reaction time in **Figure 3**. This is a product from the acid-catalyzed dehydration of glucose, as shown in reaction 7. As can be seen in the plot, the concentration of 5-HMF at 140 °C was small. However, reaction 7 became more significant as the temperature of the reactions increased. In fact, at temperatures >140 °C this dehydration reaction controlled the yield of disaccharides. As reaction 7 increased, glucose was removed from the reaction solution and the equilibrium concentration of disaccharides decreased. **Figure 4** shows the yield of disaccharides as a function of reaction time for different temperatures at a glucose concentration of 200 mg mL^{-1}. Note that at temperatures ≤140 °C, the concentration of the disaccharides increased with reaction time until equilibrium was reached, at which point the concentration remained constant with increasing reaction time. However, when the temperature was >140 °C, the concentration of the disaccharides decreased with reaction time. As can be seen,

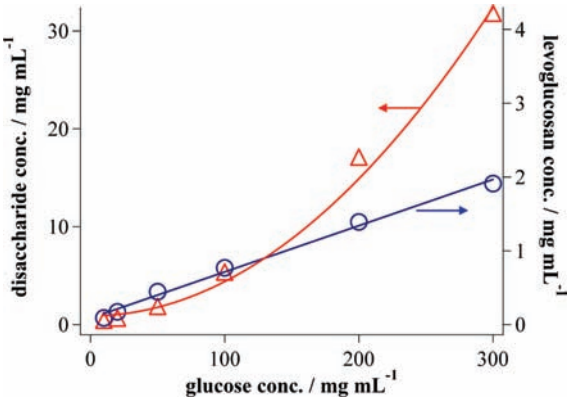

Figure 6. Formation of glucodisaccharides and levoglucosan as a function of glucose concentration. The experimental measurements (red triangles) for the disaccharides show a second-order fit (red line). The experimental measurements (blue circles) for levoglucosan show a first-order fit (blue line). These reactions were conducted at a temperature of 120 °C with H_2SO_4 concentration of 1.2 wt % and reaction time of 3600 s.

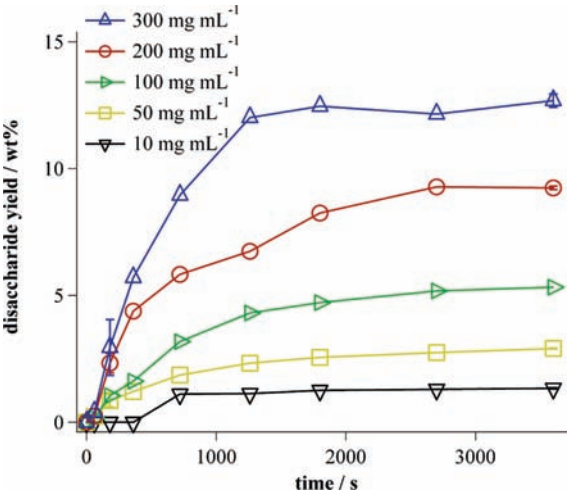

Figure 7. Conversion of glucose to disaccharides as a function of reaction time and glucose concentration. Temperature was 120 °C with H_2SO_4 concentration of 1.2 wt %.

the yield of disaccharides reached a maximum of about 10 wt % at 150 °C and 300 s.

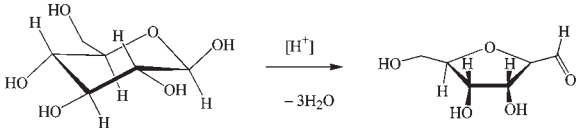

18, 5-HMF

Reaction 7

Figure 5 shows the change in glucose, disaccharides, and 5-HMF concentrations as a function of reaction time at 170 °C. As the figure shows, the concentrations of disaccharides and glucose decreased with increasing reaction time while the 5-HMF concentration increased. The glucose concentration decreased because it was undergoing the dehydration reaction, and the disaccharides concentration decreased because they were in equilibrium with glucose. That glucose and the disaccharides are at equilibrium can be seen from the equilibrium ratio $[G_2]/[G]^2$, where $[G_2]$ is the total concentration of the disaccharides and [G]

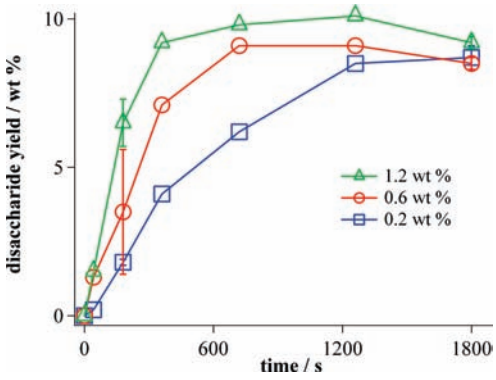

Figure 8. Effect of acid concentration and reaction time on glucodisaccharide formation. The temperature was 140 °C, the starting glucose concentration was 200 mg mL^{-1}, and the H_2SO_4 concentration was varied between 0.2, 0.6, and 1.2 wt %.

is the concentration of glucose. Note that in **Figure 5** the 5-HMF concentration leveled off at the longest reaction time. This is because the 5-HMF itself has started to decompose. At long reaction times and high temperatures, 5-HMF decomposed to formic acid and levulinic acid, as measured with HPLC, and to a polymeric material, as was evident by the formation of a brown particulate.

In addition to disaccharides concentration, the concentration of levoglucosan was measured, and the results indicate that this anhydrosugar is not a significant product compared to the disaccharides at high loadings. Data on the formation of levoglucosan are presented in **Figure 6**. From a starting glucose concentration of 300 mg mL^{-1}, the results show maximum yields of 2 mg mL^{-1} for levoglucosan and 30 mg mL^{-1} for disaccharides after 3600 s. These results suggest that anhydrosugar formation is insignificant at high substrate concentrations.

Concentration Dependence. An investigation into the concentration dependence of disaccharide formation demonstrates that the reaction is bimolecular and is consistent with the mechanisms shown in reactions 1 and 2. **Figure 7** shows the formation of disaccharides from glucose with an initial concentration ranging from 10 to 300 mg mL^{-1} at a temperature of 120 °C. Notice that for all substrate concentrations, the reaction eventually reached equilibrium, as is evident by the leveling off of the disaccharide concentrations after 2400 s. In this plot, the yield increases with concentration, confirming that the reaction is not first-order. The highest yield obtained was approximately 12 wt % at 300 mg mL^{-1} glucose loading. The reaction to form disaccharides is shown to be second-order by the graph in **Figure 6**. Here the disaccharide concentration measured after 3600 s is plotted as a function of the starting glucose concentration. The data fit well to a second-order polynomial, confirming that the reactions are dependent on the square of the glucose concentration. In contrast, the experimental measurements for levoglucosan show first-order dependence; that is, levoglucosan formation is dependent upon the glucose concentration to the first power. This is consistent with the mechanism for levoglucosan formation shown in reaction 4.

Acid Concentrations. The measured dependence of disaccharide formation on acid concentration was consistent with the mechanism shown in reactions 1 and 2. **Figure 8** shows the formation of total disaccharides from glucose as a function of reaction time for different acid concentrations. At long reaction times (1800 s), the curves converge to the same equilibrium value. However, at short reaction times, before equilibrium had been reached, an increase in acid concentration led to an increase in the rate of disaccharide formation. This indicates that acid-catalyzed

Table 2. Concentrations of α- and β-Linked Disaccharides[a]

			100 °C, 80 min (mg mL^{-1})	140 °C, 30 min (mg mL^{-1})
1,1-linked	α,α (**3**)	trehalose	0.150 ± 0.02	0.542 ± 0.008
	α,β (**4**)	neotrehalose	0.160 ± 0.03	0.300 ± 0.014
	β,β (**5**)	isotrehalose	0.400 ± 0.010	0.430 ± 0.02
1,2-linked	α (**6**)	kojibiose	1.060 ± 0.08	1.080 ± 0.04
	β (**7**)	sophorose	0.450 ± 0.08	0.700 ± 0.04
1,4-linked	α (**10**)	maltose	0.900 ± 0.10	1.088 ± 0.004
	β (**11**)	cellobiose	0.320 ± 0.04	0.700 ± 0.10
1,6-linked	α (**12**)	isomaltose	2.700 ± 0.30	5.300 ± 0.30
	β (**13**)	gentiobiose	1.900 ± 0.20	3.100 ± 0.20

[a] Starting glucose concentration of 200 mg mL^{-1}. Laminaribiose could not be quantified, and so the 1,3-linked disaccharides are not compared.

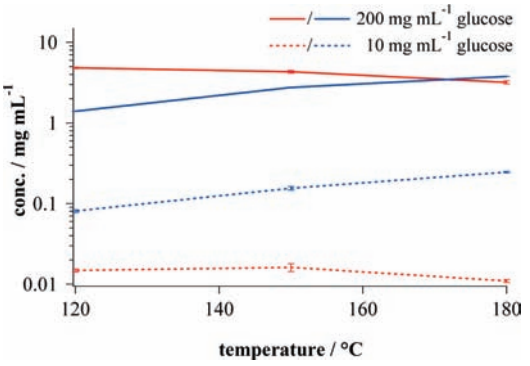

Figure 9. Comparison of the formation of gentiobiose (red lines) and levoglucosan (blue lines) from glucose at 10 and 200 mg mL^{-1} at a temperature range from 120 to 180 °C.

formation of the carbocation intermediate resulted in an increase in the rate of the reaction but did not change the equilibrium yield of the products.

Disaccharide Products. As mentioned under Materials and Methods, anion exchange chromatography with pulsed amperometric detection was used to measure the concentration of each reversion product, and experiments were conducted to determine the kinetics of formation of the reversion products. The concentrations of the disaccharide products and levoglucosan were measured at various reaction times for reaction temperatures between 100 and 140 °C. These observations are shown in **Table 2** for experiments conducted at 100 and 140 °C. Plots of the experimental results from these studies are presented later in the paper and in the Supporting Information. Consistent with literature data (*2*, *3*, *7*, *8*), these measurements show that the 1,6-linked disaccharides (isomaltose and gentiobiose) were produced at the highest yield. The data also show that the α-linked disaccharides were more abundant for each linkage studied. As can be seen in **Table 2**, the 1,6-linked disaccharides were generated at roughly 2−10 times higher yield than the other disaccharides and, with the exception of trehalose at 100 °C, the α-linked disaccharides were produced at up to twice the yield of the corresponding β isomers. The reason for this preference of 1,6-linkages and α isomers is clearly due to steric interactions, in that the two glucose rings were kept farther apart than in the other disaccharides. The α isomers were thus favored because in this orientation the linkage is axial to one ring and equatorial to the other. In the β isomers, the linkage is equatorial on both rings, creating greater steric hindrance between adjacent hydroxyl groups, which are also equatorial.

Scheme 1. Kinetic Scheme

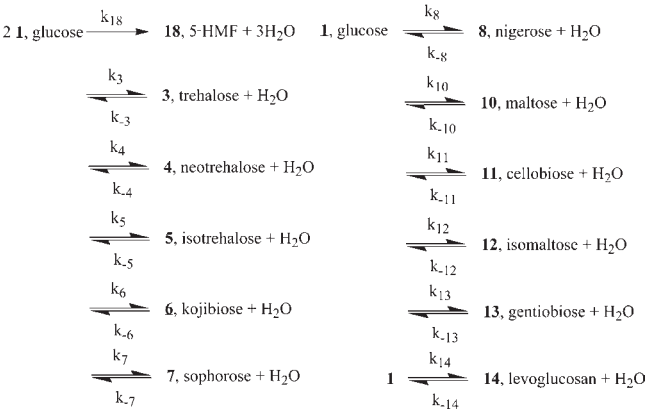

Anhydrosugars. In literature reports, anhydrosugars have been considered important reversion products from glucose, and although they were observed in this study, they were typically not produced in concentrations as high as the disaccharides formed from reversion. For example, **Figure 9** shows the formation of gentiobiose, **13**, and levoglucosan, **14**, as a function of temperature for starting glucose concentrations of 10 and 200 mg mL^{-1}. At low sugar concentrations, levoglucosan is favored, whereas at high, process-relevant concentrations (200 mg mL^{-1}) the disaccharide predominates. This is consistent with the bimolecular nature of disaccharide formation, whereas levoglucosan follows unimolecular behavior. At 10 mg mL^{-1} glucose, the levoglucosan concentration was between 5 (120 °C) and 20 (180 °C) times higher than the concentration of gentiobiose. At 200 mg mL^{-1} glucose, the gentiobiose concentration was 3 times higher than the levoglucosan concentration at 120 °C. At high temperatures (> 160 °C), the decomposition of glucose due to dehydration, reaction 7, becomes significant, and this leads to a greater reduction in gentiobiose concentration than levoglucosan concentration, because the formation of gentiobiose is dependent upon the square of the glucose concentration.

Kinetic Modeling. The kinetics of glucose reversion reactions were extracted by modeling the formation of levoglucosan and all of the disaccharides, with the exception of laminaribiose. The reaction scheme (**Scheme 1**) was used to fit measurements of glucose, the disaccharides, and levoglucosan. This scheme includes condensation reactions to form the disaccharides in addition to hydrolysis reactions of the disaccharides to reform glucose. Also included in the scheme were dehydration reactions to form levoglucosan, **14**, the hydrolysis reaction to form glucose from levoglucosan, and a dehydration reaction to form 5-HMF from glucose. In this scheme, the formation of 5-HMF was considered to be irreversible. Differential rate equations included the listed reaction rates, which were assumed to have Arrhenius temperature dependences. These differential equations were numerically solved using a fourth-order Runge−Kutta approximation (RK4). The Arrhenius parameters for the rate constants were adjusted until the calculated concentrations fit the experimental data as determined visually and by minimizing the variance between the calculated and experimental concentrations. Initial guesses for the Arrhenius parameters for some of the hydrolysis reactions were taken from the literature when possible (**Table 1**) and from separate experiments starting with disaccharides.

As mentioned above, the dehydration of glucose to form 5-HMF, **18**, by reaction 7 becomes significant at higher temperatures. It was necessary to include this reaction to obtain accurate fits of the disaccharide profiles. Kinetic parameters for this

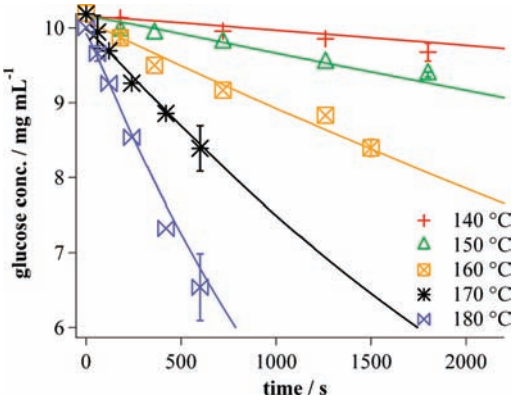

Figure 10. Fit of a first-order reaction model (lines) for reaction 7, dehydration to form 5-HMF, to the experimental decomposition of glucose (points) in 10 mg mL^{-1} solutions. Equation **1** was solved using the fourth-order Runge−Kutta approach.

reaction were extracted from independent experiments conducted starting with glucose at low concentration (10 mg mL^{-1}) to minimize the formation of disaccharides and at higher temperatures (140−180 °C) when this reaction is significant. The measured concentrations of glucose, [G], were fit to the unimolecular, first-order reaction rate equation shown in eq **1**

$$\frac{d[G]}{dt} = -k_{18}[G] \quad (1)$$

where the rate constant k_{18} was calculated using an Arrhenius relation shown in eq **2**.

$$k_{18} = A_{18} \exp\left(-\frac{E_{a18}}{RT}\right) \quad (2)$$

Equation **1** was solved analytically and numerically using the RK4 method. The analytical solution shown in eq **3** was solved by assuming that the reaction time, t, was the time at the nominal temperature (see **Figure 3**). Linear regression was used to calculate the slope (k_{18}) of ln[G] versus t for each temperature. An Arrhenius plot of ln(k_{18}) as a function of the inverse of the temperature was fit with a linear regression (see the Supporting Information), and from the slope and intercept of the line, the values of $E_{a18} = 133$ kJ mol^{-1} and $A_{18} = 1.60 \times 10^{12}$ s^{-1} were obtained.

$$\frac{[G]}{[G]_{t=0}} = \exp(-k_{18}t) \quad (3)$$

The numerical solution of eq **1** involved fitting the kinetics to the entire time/temperature profile shown in **Figure 10**. The pre-exponential factor, A_{18}, and the activation energy, E_{a18}, were adjusted until the model fit the experimental data. Because there were only two adjustable parameters, using this procedure rapidly produced a pre-exponential factor of $A_{18} = 3.4 \times 10^{12}$ s^{-1} and an activation energy of $E_{a18} = 133$ kJ mol^{-1}. **Figure 10** shows the results from the kinetic model compared to the experimental measurements for glucose. The activation energies from both approaches are similar to the value reported in the literature (*19*), E_{a18}(lit.) = 136.8 kJ mol^{-1}. Because they included reverse reaction kinetics, the parameters from the numerical solution were used in glucose reversion models without modification.

In addition to modeling the kinetics of glucose dehydration to 5-HMF, we also modeled the kinetics for dehydration of glucose to levoglucosan, because this product was formed in the same yield as some of the disaccharides and standards were readily available. To obtain independent kinetic parameters for this reaction, experiments were conducted with (1) 10 mg mL^{-1} glucose in 1.2 wt % acid and (2) 10 mg mL^{-1} levoglucosan in 1.2 wt % acid. At these concentrations, interference from disaccharide formation was minimized. The levoglucosan was measured as a function of reaction time at low temperatures, 100−140 °C, which minimized dehydration to 5-HMF, reaction 7. As with the glucose reversion reactions that form disaccharides, this reaction is reversible and equilibrium is established between levoglucosan and glucose. As a result, it was only possible to analytically model the conversion of levoglucosan to glucose at low conversion, when minimal glucose was produced. Under these conditions, the reverse reactions were minor and the kinetics could be modeled using a simplification of eq **4** below, where [L] is the concentration of levoglucosan. In experiments starting with glucose, it was not possible to use an analytical solution to the kinetics because the conversion of glucose was low. The analytical fits are shown in graphs in the Supporting Information, and the fit parameters are collected in **Table 3**. The full differential equations for levoglucosan to glucose are shown in eqs **4** and **6** and were used for numerically modeling the data. The water concentration was assumed to be the density of pure water, 1 g mL^{-1}. Equation **7** shows the Arrhenius parameters for the rate constants in eqs **4** and **6**. These parameters were adjusted until reasonable fits to the experimental data were obtained. **Figure 11** shows the fit of this model to the data. The parameters obtained from this fit were $A_{14} = 1.3 \times 10^{18}$ s^{-1}, $E_{a14} = 170$ kJ mol^{-1}, $A_{-14} = 8.0 \times 10^{14}$ mL g^{-1} s^{-1}, and $E_{a-14} = 130$ kJ mol^{-1}.

$$\frac{d[L]}{dt} = k_{14}[G] - k_{-14}[L][H_2O] \quad (4)$$

$$\frac{d[L]}{dt} = -k_{-14}[L][H_2O] \qquad [G] \rightarrow 0 \quad (5)$$

$$\frac{d[G]}{dt} = k_{-14}[L][H_2O] - k_{14}[G] \quad (6)$$

$$k_{14} = A_{14} \exp\left(-\frac{E_{a14}}{RT}\right), k_{-14} = A_{-14} \exp\left(-\frac{E_{a-14}}{RT}\right) \quad (7)$$

Some of the kinetic parameters for disaccharides were taken from the literature (see **Table 1**) or were experimentally determined by measuring their hydrolysis rates. Hydrolysis kinetics were measured for trehalose, **3**, maltose, **10**, and cellobiose, **11**. These experiments were conducted between 100 and 140 °C with starting disaccharide concentrations of 10 mg mL^{-1}. At these low concentrations the disaccharides were hydrolyzed to give glucose, with minimal recombination of the glucose to re-form disaccharides. Parenthetically, when experiments were conducted starting with high concentrations (200 mg mL^{-1}) of a single disaccharide, glucose and the other disaccharides were found in abundance. For each of the disaccharides studied, an analytical first-order model was used to extract Arrhenius parameters (such as eq **3**) and a numerical model was used to fit the data. **Figure 12** shows results from the numerical model for cellobiose hydrolysis and glucose formation, respectively. The model curves in these graphs were generated by numerically solving eqs **8** and **9**, where [C] is the concentration of cellobiose. These equations are valid at low cellobiose concentrations because reversion reaction rates to form disaccharides are negligible. The Arrhenius parameters for k_{11} and k_{-11} were adjusted until the model curves fit the experimental

Table 3. Kinetic Parameters Obtained by Modeling Disaccharide Formation

reaction		A (s^{-1})	E_a (kJ mol^{-1})	lit. E_a (kJ mol^{-1})
1, glucose → **18**, 5-HMF + $3H_2O$	k_{18}	3.4×10^{12}	133	136.8[a]
		(1.6×10^{12})[b]	(133)[b]	
		(3.4×10^{12})[c]	(133)[c]	
⇌ **14**, levoglucosan + H_2O	k_{14}	3.6×10^{17}	170	
		(1.3×10^{18})[c]	(170)[c]	
reaction		A (mL g^{-1} s^{-1})	E_a (kJ mol^{-1})	lit. E_a (kJ mol^{-1})
	k_{-14}	2.8×10^{14}	130	
		(1.8×10^{13})[b]	(118)[b]	
		(8.0×10^{14})[c]	(130)[c]	
⇌ **3**, trehalose + H_2O	k_3	5.0×10^{16}	163	
	k_{-3}	9.0×10^{17}	159	168.1[d]
		(7.6×10^{17})[b]	(160)[b]	
		(4.5×10^{17})[c]	(159)[c]	
⇌ **4**, neotrehalose + H_2O	k_4	1.9×10^{11}	124	
	k_{-4}	1.1×10^{14}	129	
⇌ **5**, isotrehalose + H_2O	k_5	1.1×10^{12}	125	
	k_{-5}	3.0×10^{14}	129	
⇌ **6**, kojibiose + H_2O	k_6	3.0×10^{13}	133	
	k_{-6}	4.8×10^{15}	139	
⇌ **7**, sophorose + H_2O	k_7	8.5×10^{10}	117	
	k_{-7}	7.8×10^{12}	120	
⇌ **8**, nigerose + H_2O	k_8	4.3×10^{11}	121	
	k_{-8}	5.0×10^{13}	113	
⇌ **10**, maltose + H_2O	k_{10}	1.3×10^{15}	145	
	k_{-10}	1.2×10^{16}	141	132.0[e]
		(1.5×10^{15})[b]	(136)[b]	129.6[f]
		(1.0×10^{16})[c]	(141)[c]	
⇌ **11**, cellobiose + H_2O	k_{11}	1.4×10^{13}	134	
	k_{-11}	4.0×10^{14}	129	129.0[e]
		(5.3×10^{13})[b]	(123)[b]	128.4[f]
		(5.3×10^{14})[c]	(132)[c]	130.0[g]
⇌ **12**, isomaltose + H_2O	k_{12}	1.4×10^{14}	136	
	k_{-12}	5.3×10^{15}	142	
⇌ **13**, gentiobiose + H_2O	k_{13}	1.8×10^{14}	137	
	k_{-13}	6.5×10^{15}	142	

[a] Determined using an analytical solution to the rate equations as discussed in the text. [b] Determined using a numerical solution to the rate equations as discussed in the text. [c] Reference *19*. [d] Reference *20*. [e] Reference *13*. [f] Reference *21*. [g] Reference *22*.

data points. Plots for the other starting materials and the analytical fits are presented in the Supporting Information, and **Table 3** lists the Arrhenius parameters determined from both the analytical and numerical solutions.

$$\frac{d[C]}{dt} = k_{-11}[G]^2 - k_{11}[C][H_2O] \quad (8)$$

$$\frac{d[G]}{dt} = 2k_{11}[C][H_2O] - 2k_{-11}[G]^2 \quad (9)$$

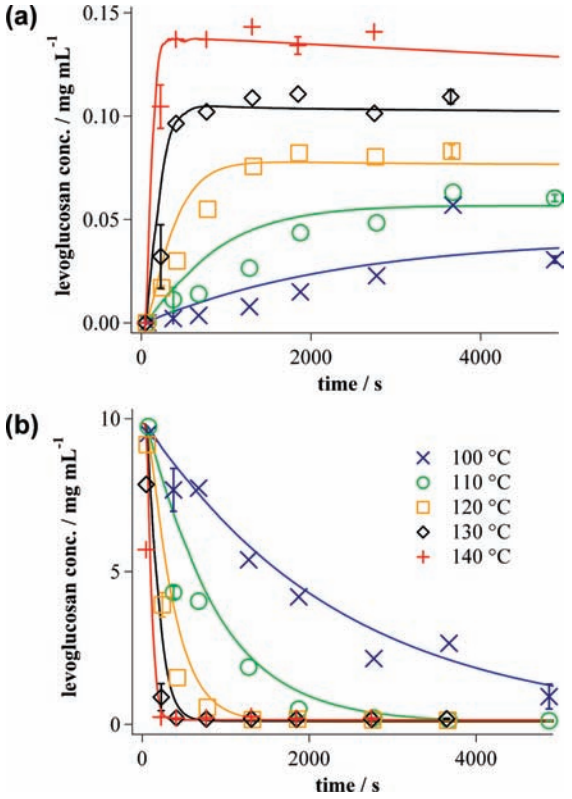

Figure 11. Fits of eqs **4** and **6** to experimental levoglucosan concentration data for (**a**) the reaction of glucose to levoglucosan (10 mg mL^{-1} solution of glucose in 1.2 wt % H_2SO_4) and (**b**) reaction of levoglucosan to glucose (10 mg mL^{-1} solution of levoglucosan in 1.2 wt % H_2SO_4).

Reaction Kinetics of Glucose Reversion Reactions. Finally, numerical models were used to fit the kinetic data for the conversion of glucose to disaccharides and levoglucosan as a function of reaction time and temperature. The goal was to model the loss of glucose and the formation of all of the individual reversion products. The model results were refined by comparing them to the experimental measurements obtained when a 200 mg mL^{-1} glucose solution was reacted in 1.2 wt % H_2SO_4. As shown in the kinetic modeling scheme above, 11 reversion reactions were considered in this model. The dehydration of glucose to give 5-HMF was added for completeness. The rate of decomposition of glucose was described by eq **10**, where k_{18} is the rate constant for dehydration to 5-HMF. The sum $(2k_3 + ... + k_{13})$ contains the rate constants for the reversion reactions, and the sum $(2k_{-3}[T][H_2O] + ... + k_{-14}[L][H_2O])$ contains the rates for hydrolysis of the disaccharides and levoglucosan, where [T] is the concentration of trehalose and [L] is the concentration of levoglucosan. Examples of the differential equations describing the formation of the disaccharides and levoglucosan and the Arrhenius relations are shown in eqs **11** and **12**. There are 23 pre-exponential factors and activation energies that describe this model. To obtain the time courses for glucose and the disaccharides obtained during glucose reversion, eqs **10** and **11** were integrated numerically using RK4. The parameters obtained from measuring the dehydration of glucose to 5-HMF were fixed at the values obtained from the model shown in **Figure 10**. Initial hydrolysis reaction rate constant parameters were taken either from the experimental results discussed above or from literature values. The forward reversion rate parameters were adjusted to obtain a rough fit to the

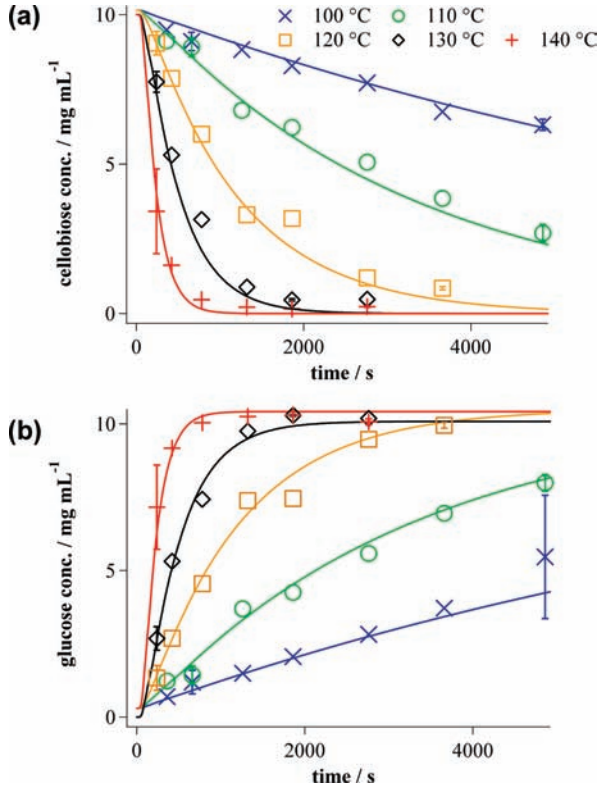

Figure 12. Fits of the kinetic model to experimental data from a reaction of cellobiose to glucose for (**a**) cellobiose hydrolysis and (**b**) formation of glucose.

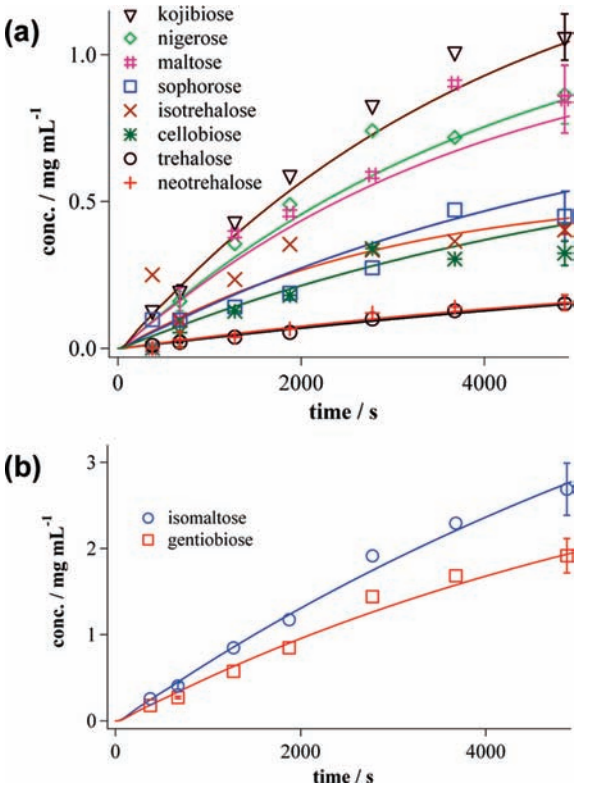

Figure 13. Fits of the kinetic model to experimental data from a reaction of glucose to disaccharides for (**a**) 1,1- to 1,4-linked disaccharides and (**b**) 1,6-linked disaccharides. This was from an experiment using 200 mg mL^{-1} glucose in 1.2 wt % H_2SO_4 at 100 °C.

data, and then all of the rate parameters for forward and reverse reactions were adjusted.

$$\frac{d[G]}{dt} = -(k_{14} + k_{18})[G] - (2k_3 + ... + k_{13})[G]^2 + 2k_{-3}[T][H_2O] + ... + k_{-14}[L][H_2O] \quad (10)$$

$$\frac{d[T]}{dt} = k_3[G]^2 - k_{-3}[T][H_2O]$$
$$\bullet$$
$$\bullet$$
$$\bullet \quad (11)$$
$$\frac{d[L]}{dt} = k_{14}[G] - k_{-14}[L][H_2O]$$

$$k_3 = A_3 \exp\left(-\frac{E_{a3}}{RT}\right)$$
$$\bullet$$
$$\bullet$$
$$\bullet \quad (12)$$
$$k_{-14} = A_{-14} \exp\left(-\frac{E_{a-14}}{RT}\right)$$

The kinetic equations, eqs **11** and **12**, used in this work were fitted to the experimental data by minimization of the sum of the square of the deviation between model prediction and experimental data. The pre-exponential factors (A_{18}, A_3, ..., A_{-14}) and the activation energies (E_{a18}, E_{a3}, ..., E_{a-14}) for the disaccharide reversion products formed during glucose hydrolysis were then obtained from data collected at low temperatures (100−140 °C) and high concentration (200 mg mL^{-1}) using the equations in eq **11**. The resulting fits for the formation of the disaccharides are shown in **Figure 13** for experiments conducted at 100 °C. The theoretical fits to the rest of the experimental data are shown in the Supporting Information. The kinetic parameters obtained by fitting the model to the experimental data are shown in **Table 3**.

In summary, experimentation and kinetic modeling have demonstrated that reversion reactions of glucose to produce disaccharides can play a significant role at high concentrations and low temperatures. Anhydrosugar formation, principally to levoglucosan, is more important at low glucose concentrations, due to their first-order reactions. Arrhenius activation energies and pre-exponential factors were derived from modeling kinetic data, and these models can ultimately be used to predict the formation of the glucodisaccharides as a function of reaction time and temperature.

ABBREVIATIONS USED

nC, nanocoulomb; k rate constant (s^{-1}); A, Arrhenius constant (s^{-1}); E_a, activation energy, kJ mol^{-1}; R, universal gas constant, 8.314×10^{-3} kJ mol^{-1} K^{-1}; T, temperature, Kelvin, K; t, time, s; $\Delta_r G°$, free energy of the reaction, kJ mol^{-1}; $\Delta_r H°$, enthalpy, kJ mol^{-1}.

Supporting Information Available: Table S1 (full names and chemical structures of the disaccharides identified from glucose reversion reactions) and Figures S1−S13. This material is available free of charge via the Internet at http://pubs.acs.org.

LITERATURE CITED

(1) Silberman, H. Reactions of sugars in the presence of acids: a paper chromatographic study. *J. Org. Chem.* **1961**, *26*, 1967–1969.
(2) Minor, J. L., Nonfermentable, glucose-containing products formed from glucose under cellulose acid hydrolysis conditions. *J. Appl.*

Polym. Sci.: Appl. Polym. Symp. **1983**, *37* (Proc. Cellul. Conf., 9th, 1982, Part 2), 617−629.
(3) Peat, S.; Whelan, J.; Edwards, T. E.; Owen, O. Quantitative aspects of the acid reversion of glucose. *J. Chem. Soc.* **1958**, 586–592.
(4) Smith, P. C.; Grethlein, H. E.; Converse, A. O. Glucose decomposition at high temperature, mild acid, and short residence times. *Sol. Energy* **1982**, *28* (1), 41–48.
(5) Thompson, A.; Anno, K.; Wolfrum, M.; Inatome, M. Acid reversion products from D-glucose. *J. Am. Chem. Soc.* **1954**, *76*, 1309–1311.
(6) Vandam, H. E.; Kieboom, A. P. G.; Vanbekkum, H. The conversion of fructose and glucose in acidic media − formation of hydroxymethylfurfural. *Starch/Staerke* **1986**, *38* (3), 95–101.
(7) Helm, R. F. Reversion and dehydration reactions of glucose during the dilute sulfuric acid hydrolysis of cellulose. Ph.D. Dissertation, University of Wisconsin, Madison, WI, **1987**.
(8) Helm, R. F.; Young, R. A.; Conner, A. H. The reversion reactions of D-glucose during the hydrolysis of cellulose with dilute sulfuric acid. *Carbohydr. Res.* **1989**, *185* (2), 249–260.
(9) Ball, D. H.; Jones, J. K. N. The acid-catalysed reversion of D-xylose. *J. Chem. Soc.* **1958**, 33–36.
(10) Jacobsen, S. E.; Wyman, C. E. Cellulose and hemicellulose hydrolysis models for application to current and novel pretreatment processes. *Appl. Biochem. Biotechnol.* **2000**, *84* (6), 81–96.
(11) Mosier, N.; Wyman, C.; Dale, B.; Elander, R.; Lee, Y. Y.; Holtzapple, M.; Ladisch, M. Features of promising technologies for pretreatment of lignocellulosic biomass. *Bioresour. Technol.* **2005**, *96* (6), 673–686.
(12) Xiang, Q.; Lee, Y. Y.; Torget, R. W. Kinetics of glucose decomposition during dilute-acid hydrolysis of lignocellulosic biomass. *Appl. Biochem. Biotechnol.* **2004**, *113*, 1127–1138.
(13) Wolfrom, M. L.; Thompson, A.; Timberlake, C. E. Comparative hydrolysis rates of the reducing disaccharides of D-glucopyranose. *Cereal Chem.* **1963**, *40*, 82–86.
(14) Girisuta, B.; Janssen, L.; Heeres, H. J. A kinetic study on the conversion of glucose to levulinic acid. *Chem. Eng. Res. Des.* **2006**, *84* (A5), 339–349.
(15) Sasaki, M.; Takahashi, K.; Haneda, Y.; Satoh, H.; Sasaki, A.; Narumi, A.; Satoh, T.; Kakuchi, T.; Kaga, H. Thermochemical transformation of glucose to 1,6-anhydroglucose in high-temperature steam. *Carbohydr. Res.* **2008**, *343* (5), 848–854.
(16) Goldberg, R. N.; Bell, D.; Tewari, Y. B.; McLaughlin, M. A. Thermodynamics of hydrolysis of oligosaccharides. *Biophys. Chem.* **1991**, *40*, 69–76.
(17) Tewari, Y. B.; Goldberg, R. N. Thermodynamics of hydrolysis of disaccharides. *J. Biol. Chem.* **1989**, *264*, 3966–3971.
(18) Tewari, Y. B.; Goldberg, R. N. Thermodynamics of hydrolysis of disaccharides lactulose, α-D-melibiose, palatinose, D-trehalose, D-turanose and 3-*O*-β-D-galactopyranosyl-D-arabinose. *Biophys. Chem.* **1991**, *40*, 59–67.
(19) McKibbins, S. W.; Harris, J. F.; Saeman, J. F.; Neil, W. K. Kinetics of the acid catalyzed conversion of glucose to 5-hydroxymethyl-2-furaldehyde and levulinic acid. *For. Prod. J.* **1962**, 17–23.
(20) Moelwyn-Hughes, E. A. Part II. Trehalose, α-methylglucoside and tetramethyl-α-mehylglucoside. *Trans. Faraday Soc.* **1929**, *25*, 81–92.
(21) Moelwyn-Hughes, E. A. Part III. β-Methylglucoside, cellobiose, melibiose, and turanose. *Trans. Faraday Soc.* **1929**, *25*, 503–520.
(22) Sharples, A. The hydrolysis of cellulose and its relation to structure. *Trans. Faraday Soc.* **1957**, *53*, 1003–1013.

Received for review October 15, 2009. Revised manuscript received January 27, 2010. Accepted January 29, 2010. Funding for this research was provided by the U.S. Department of Energy, Office of the Biomass Program.